SCIENTIFIC ARTICLE

Extensor retinaculum of the wrist: gross anatomical correlation with MR imaging after ultrasound-guided tenography with emphasis on anatomical features in wrist dorsiflexion responsible for tendon impingement

Alexandre Norio Massaki · Jeffrey Tan ·
Brady K. Huang · Eric Y. Chang · Debra J. Trudell ·
Donald L. Resnick

Abstract

Objective To demonstrate the anatomy of the extensor retinaculum (ER) of the wrist using gross anatomical correlation with magnetic resonance (MR) imaging before and after ultrasound-guided tenography in four different positions, emphasizing the morphological appearance of the ER that occurs with dorsiflexion of the wrist to define the nature of extensor tendon impingement in athletes who perform repetitive wrist dorsiflexion.

Materials and methods Institutional policies were followed regarding cadaver use. Ten upper extremities were harvested from fresh cadavers. MR imaging before and after ultrasound-guided tenography of the wrist was performed, followed by gross anatomical correlation. Two radiologists interpreted the MR images and sections by consensus for the anatomical landmarks of the ER, and morphological changes occurring during dorsiflexion of the wrist were analyzed and measured.

Results The ER of the wrist appeared as a band of low signal intensity on T1- and PD-weighted images. Because of its orientation, axial images were best suited to depict the ER anatomy; specifically, localization of the bony landmarks and the septal attachments. On sagittal images, a consistent appearance of the ER was seen: appearing with fusiform morphology in the neutral position, and becoming shortened and thickened at the abutment point where the extensor tendons of the fourth compartment had a curved excursion during dorsiflexion. The width and thickness of the ER in neutral position averaged 13.56 mm and 1.67 mm respectively. In wrist dorsiflexion, the average width and thickness changed to 8.68 mm and 2.15 mm respectively.

Conclusion Magnetic resonance imaging is a useful technique to demonstrate the ER of the wrist, the septal attachments, and morphological changes that occur during dorsiflexion of the wrist, which potentially can lead to impingement of the extensor tendons.

Keywords Magnetic resonance imaging · Tenography · Wrist · Extensor retinaculum · Tendon impingement · Extensor compartments

A. N. Massaki · J. Tan · B. K. Huang · E. Y. Chang · D. L. Resnick
Department of Radiology, Division of Musculoskeletal Radiology, University of California, San Diego—UCSD Teleradiology and Education Center, La Jolla, CA, USA

A. N. Massaki · J. Tan · E. Y. Chang · D. J. Trudell
VA San Diego Healthcare System, San Diego, La Jolla, CA, USA

A. N. Massaki (✉)
Department of Radiology, Santa Casa de Votuporanga, Rua Minas Gerais, 3051, 15500-003 Votuporanga, SP, Brazil
e-mail: anmassaki@gmail.com

Introduction

The extensor retinaculum (ER) of the wrist is an important and complex structure that has been well described as a thickening of the distal antebrachial fascia at the level of the inferior radioulnar joint that involves the extensor tendons over the radial, dorsal, and ulnar aspects of the wrist, preventing their bowstringing [1]. It consists of two layers: the supratendinous retinaculum and the infratendinous retinaculum [2]. It can be used, together with its septal attachments, as an autogenous graft for ligament or pulley reconstructions [3, 4]. The ER has also been rarely reported as a cause of impingement of the extensor tendons as a result of an anomalous muscle, intratendinous lesion, or synovial inflammation and tendon fraying [5]. Such impingement contributes to overuse

syndromes in sporting activities that require repetitive dorsiflexion of wrists, such as gymnastics, weightlifting, shot putting and platform diving [6, 7].

Although the anatomy of the ER has been well described, to our knowledge there are no studies correlating this anatomy to images provided by magnetic resonance (MR), ultrasound, and gross anatomical sections. In addition, there are no previous studies demonstrating the morphological changes of the ER that occur during dorsiflexion of the wrist, which may contribute to ER impingement of the extensor tendons in certain athletes.

The purpose of our study is to define the anatomy of the ER of the wrist using cadaveric specimens and to correlate this anatomy with MR imaging before and after ultrasound-guided tenography, with particular attention to the radial and ulnar retinacular attachments and to morphological changes occurring with dorsiflexion of the wrist that might explain the pathogenesis of extensor tendon impingement in athletes who perform repetitive wrist dorsiflexion.

Materials and methods

This cadaveric study did not require institutional review board approval or informed consent according to the rules of the hospital where the study was performed.

Specimens

Ten upper extremities were harvested from fresh cadavers (7 men and 3 women, 53 to 91 years of age at death, mean 77.5 years). The arms were transected proximal to the elbow joint, and immediately deep-frozen at −40 °C (Forma BioFreezer; Forma Scientific, Marietta, OH, USA). All specimens were allowed to thaw at room temperature at least 24 h before performing ultrasound-guided tenography and MR imaging.

MR imaging

Magnetic resonance imaging was performed with a 1.5-T MR system (Signa; GE Medical Systems, Milwaukee, WI, USA) and a dedicated eight-channel phased array knee coil. Each of the 10 specimens were imaged with the wrist in four different positions: neutral position, supination, pronation, and dorsiflexion. To ensure the correct positioning, a custom-built 90° device was used to keep the arm fixed during full supination and pronation, and to keep the hand dorsiflexed as close as possible to a 90° angle.

T1-weighted spin-echo non-fat-saturated (500/14 [repetition time ms/echo time ms]; matrix, 384×288; field of view, 7×5.25 cm; slice thickness, 2.0 mm; interslice gap, 0.6 mm; number of excitations, six; bandwidth, 19.23), and proton density (PD)-weighted fast spin-echo non-fat-saturated (1, 800/6 [repetition time ms/echo time ms]; matrix, 512×320; field of view 8×5.6 cm; slice thickness, 2.0 mm; interslice gap, 0.4 mm; number of excitations, six; bandwidth, 19.23; echo train length, three) images were acquired in axial (all positions) and sagittal (neutral position and dorsiflexion) planes.

Tenography

After MR imaging of all 10 specimens, 5 were subjected to tenography utilizing ultrasound guidance (Acuson Sequoia 512 and Acuson S2000; Siemens, Mountain View, CA, USA). Approximately 2–4 mL of a solution consisting of 2 mL of gadopentetate dimeglumine (Magnevist; Schering, Berlin, Germany) diluted in 400-mL equal parts of saline solution and iodinated contrast agent (Iohexol, Omnipaque 350; Bayer Healthcare Pharmaceuticals, Leverkusen, Germany) with a mixture of gelatin was injected via a 20-gauge needle from a dorsal approach utilizing ultrasound guidance into the fourth and sixth extensor compartments. To access the fourth extensor compartment, the needle was placed proximal to the ER for the injection. To access the sixth extensor tendon
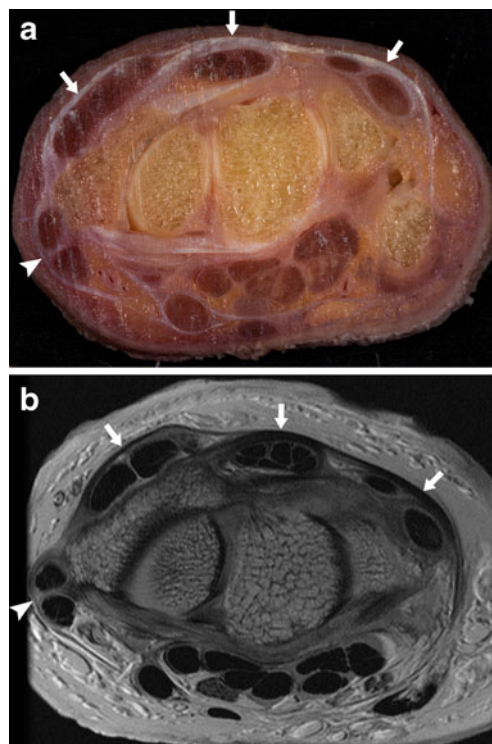

Fig. 1 Extensor retinaculum (ER) of the wrist. **a** Axial gross anatomical section and **b** corresponding proton density (PD)-weighted image at the level of the radioulnar joint show the ER of the wrist (*arrows*) located dorsal to the tendons of the extensor muscles, as a band of low signal intensity on PD-weighted images. In some cases, the septum (*arrowhead*) can be found separating the abductor pollicis longus and extensor pollicis brevis tendons

compartment, the needle was placed proximal to the base of the ulnar styloid between the extensor carpi ulnaris (ECU) tendon and its subsheath for the injection. The maximum volume injected into each of the fourth and sixth extensor compartments was 4 mL respectively.

Repeat MR imaging after tenography of the five specimens was accomplished again using the same positions, and the following protocol: T1-weighted spin-echo fat-saturated (500/14 [repetition time ms/echo time ms]; matrix, 384×288; field of view, 7×5.25 cm; slice thickness, 2.0 mm; interslice gap, 0.6 mm; number of excitations, two; bandwidth, 3.01), and PD-weighted fast spin-echo non-fat-saturated (1,800/6 [repetition time ms/echo time ms]; matrix, 512×320; field of view 8×5.6 cm; slice thickness, 2.0 mm; interslice gap, 0.4 mm; number of excitations, six; bandwidth, 19.23; echo train length, three).

Anatomical section

After imaging, the specimens were deep frozen again for at least 24 h. Four of the specimens were frozen in neutral position, two in supination, two in pronation and two in dorsiflexion. A bandsaw was used to slice the specimens into 3-mm-thick sections, corresponding closely to the plane and thickness of the MR images. Five specimens were sectioned in the axial plane (1 in neutral position, 2 in supination [1 after tenography], and 2 in pronation [1 after tenography]), and 5 in the sagittal plane (3 in neutral position [2 after tenography], and 2 in dorsiflexion [1 after tenography]). For the dorsiflexion position, the same custom-built 90° device used during the MR imaging was employed during the freezing process. Each slice was digitally photographed (Nikon D5000; Nikon Corp., Ayutthaya, Thailand) and radiographed with a high-resolution radiographic unit (Faxitron; Hewlett Packard, McMinnville, OR, USA).
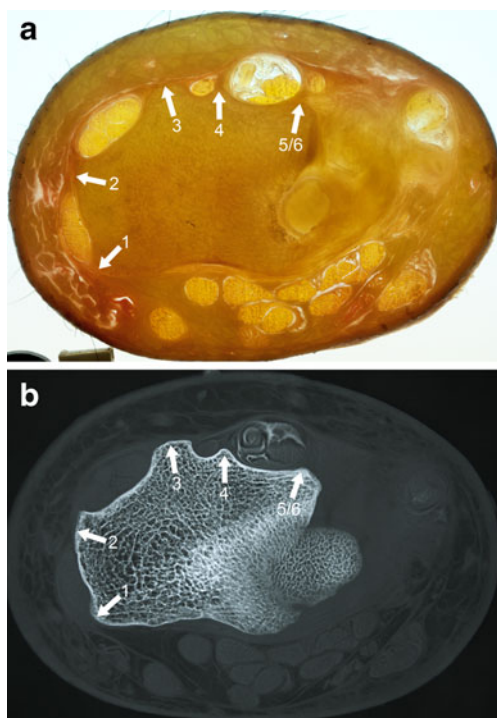

Fig. 2 Septal attachments of the ER. **a** Axial gross anatomical section, and **b** corresponding high-resolution radiograph at the level of the distal radius show bony landmarks (*arrows*) of the six ER septal attachments on the radius (*numbered*). Contrast material distends the fourth and sixth extensor compartments
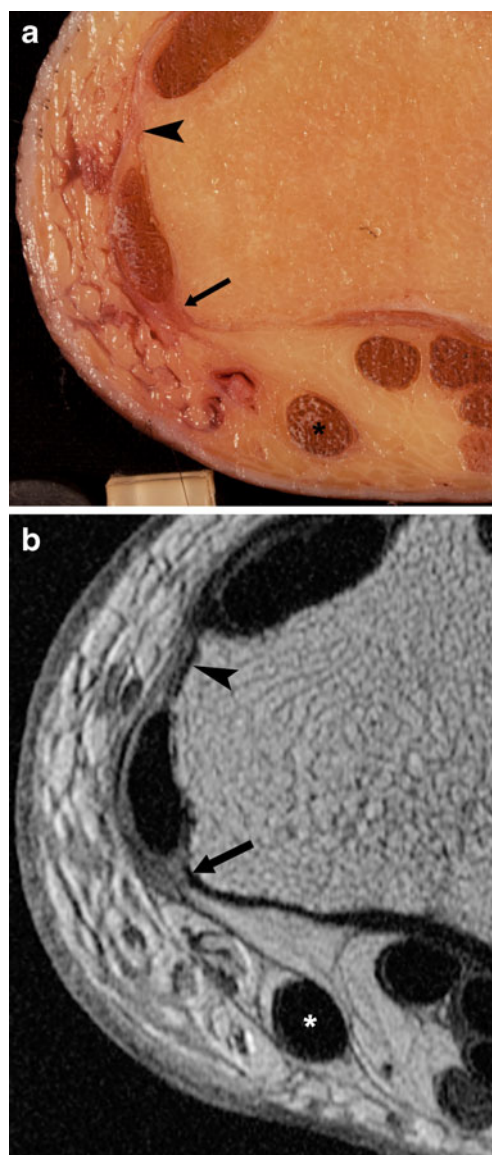

Fig. 3 First extensor compartment (abductor pollicis longus, extensor pollicis brevis tendons). **a** Axial gross anatomical section, and **b** corresponding PD-weighted image, show the first (*arrow*) and second (*arrowhead*) septal attachments of the ER over the first extensor compartment. The ER continues volarly to blend with the volar antebrachial fascia and invests the flexor carpi radialis tendon (*asterisk*)
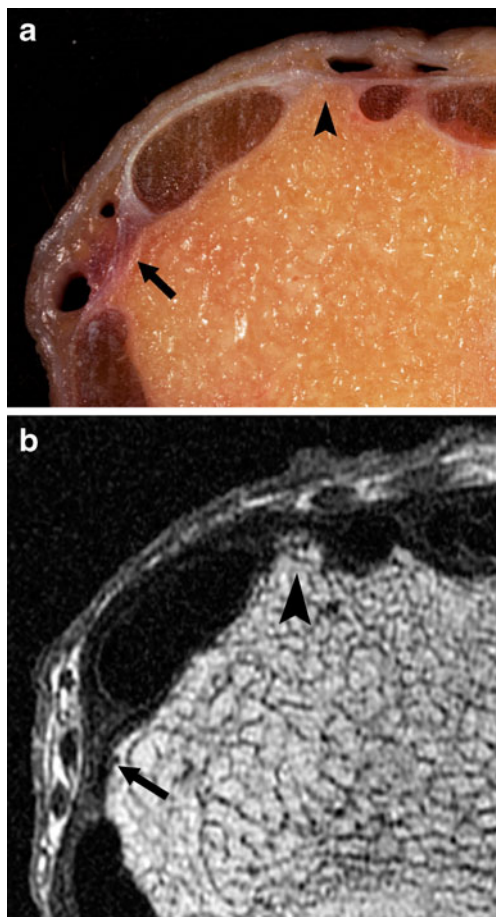
Fig. 4 Second and third extensor compartments (extensor carpi radialis longus/brevis and extensor pollicis brevis tendons). **a** Axial gross anatomical section, and **b** corresponding T1-weighted image show the second septal attachment (*arrow*) and the third septal attachment of the ER at Lister's tubercle (*arrowhead*)

Fig. 5 Fourth extensor compartment (extensor digitorum communis, extensor indicis proprius tendons). **a** Axial gross anatomical section after tenography, **b** corresponding PD-weighted image, and **c** ultrasound image without tenography show the fourth septal attachment (*arrowhead*) of the supratendinous (*black arrow*) and infratendinous (*white arrow*) portions of the ER to the radius. The shape and hypoechogenicity from anisotropy in relation to adjacent tendons on ultrasound can be misdiagnosed as fluid

Measurements and evaluation on MR and ultrasound images, gross slices, and high-resolution radiographs

All MR and ultrasound images, gross anatomical slices, and high-resolution radiographs were evaluated retrospectively by two musculoskeletal radiologists (A.N.M. and J.T.; 6 years and 1 year of experience respectively in musculoskeletal imaging) by consensus. MR and ultrasound images were reviewed using Amicas PACS software (Merge Healthcare Solutions, Boston, MA, USA).

Regarding the anatomical landmarks of the ER of the wrist, its 6 septal osseous attachments to the radius were localized and described using MR images and correlated with gross sections and radiographs, as well as its ulnar and radial side attachments and its relationship to the ECU subsheath. Comparison between sagittal MR images during neutral and dorsiflexion positions of the wrist was performed to evaluate the morphological changes of
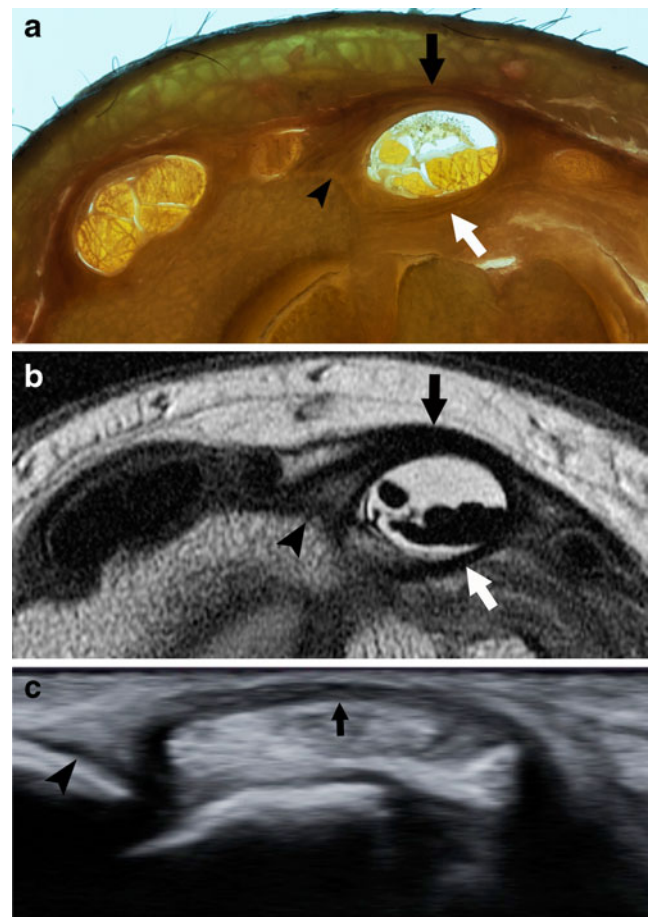
the ER at the level of the fourth extensor tendon compartment, and then correlated with anatomical section slices, radiographs, and dynamic ultrasound. We performed a dynamic study utilizing ultrasound, dorsiflexing the wrist while keeping the transducer in a sagittal position over the fourth compartment. We could not completely dorsiflex the wrist to the desired 90° angle owing to the constrained space in the dorsiflexed wrist, despite using the small footprint of a hockey stick transducer.

After determining the level of the central portion of the fourth compartment using MR axial images, the corresponding cross-referenced sagittal image was used to measure the largest width and thickness of the ER in neutral and in dorsiflexion positions. Statistical differences were analyzed by paired, two-tailed Student's t test, and a value of $p < 0.05$ was regarded as statistically significant,

Fig. 6 Fifth extensor compartment (extensor digiti minimi tendon). **a** Axial gross anatomical section after tenography, and **b** corresponding T1-weighted fat-saturated image demonstrating the common attachment of the fifth and sixth septa (*arrow*) at the dorsoulnar aspect of the radius (*R*), adjacent to the ulna (*U*). **c** Axial gross anatomical slice, and **d** corresponding PD-weighted image demonstrating separate osseous attachments of the fifth and sixth septa to the radius (*arrowheads*), but in a very close relationship to each other. The supratendinous and infratendinous portions of the ER continue around the extensor digiti minimi tendon (*asterisk*), forming the fifth compartment
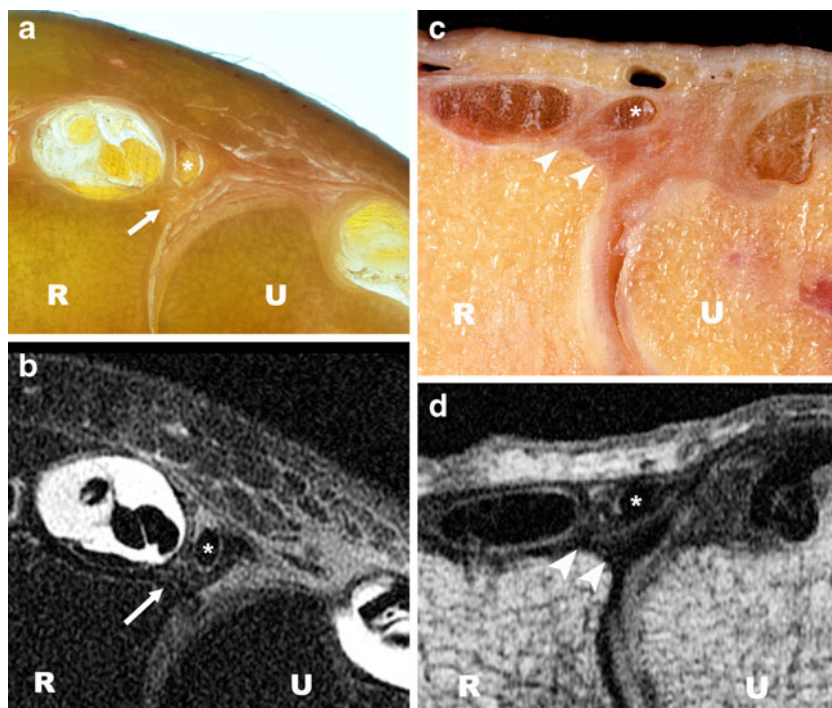
using Microsoft Excel for Mac 2011 (Microsoft, Redmond, WA, USA).

The largest width (craniocaudal) and thickness (anteroposterior) of the ER were measured using electronic calipers on sagittal MR images before tenography. In order to determine the sagittal level to be used for the measurements and evaluation of the morphological changes of the ER, the central portion of the fourth compartment was defined on the axial images, and then cross-referenced to the respective sagittal image, for both neutral and dorsiflexion positions. During a preliminary review of our data images, the central portion of the fourth extensor compartment was chosen because the retinaculum appeared thickest at this level and optimal for evaluation of changes occurring during wrist dorsiflexion, as well as for measurements. Moreover, this compartment was often affected according to previous studies describing ER impingement of the wrist [5–7].

Results

Anatomy

The ER of the wrist, a thickened component of the antebrachial fascia that lay obliquely over the extensor tendons of the wrist at the level of the radioulnar joint, appeared as a band of low signal intensity on T1 and PD-weighted images (Fig. 1). Because of its orientation, axial images were best suited to depict the ER anatomy; specifically, the localization of the bony landmarks and its septal attachments (Fig. 2).

First compartment (abductor pollicis longus and extensor pollicis brevis tendons)

The proximal attachment of the ER, which is also considered the first septal attachment, began on the radial side of the wrist, where it inserted into the radius at the volar–radial border above the styloid process, and also blended with the volar antebrachial fascia and involved the flexor carpi radialis tendon. The ER crossed over the abductor pollicis longus (APL) and extensor pollicis brevis (EPB) tendons to attach to the second septal attachment, a dorsoradial bony protuberance on the distal radius that separated the first from the second compartment (Fig. 3).

In only 1 of the 10 cases of our study we found an individual septum intrinsic to the first dorsal compartment separating the APL and EPB tendons.

Second compartment (extensor carpi radialis longus and extensor carpi radialis brevis tendons)

The ER crossed over the extensor carpi radialis longus and extensor carpi radialis brevis tendons, from its second septal attachment to its third septal attachment at Lister's tubercle, an important osseous landmark that separated the second and third compartments, where it had an extensive attachment (Fig. 4).
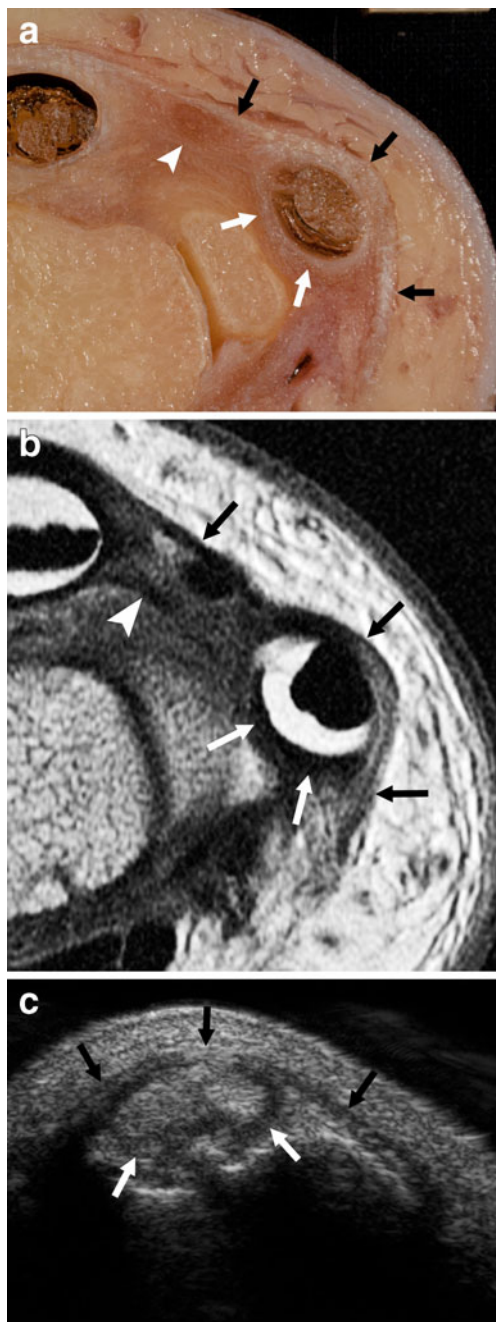
Fig. 7 Sixth extensor compartment (extensor carpi ulnaris tendon). **a** Axial gross anatomical section after tenography, **b** corresponding PD-weighted image, and **c** ultrasound image show that the ECU tendon is invested by its own fibrous subsheath (*white arrows*), derived from the pars profunda of the antebrachial fascia specifically formed by the infratendinous retinaculum (*arrowhead*). The supratendinous portion of the ER (*black arrows*) crosses over the ECU tendon and its subsheath

Third compartment (extensor pollicis longus tendon)

The third compartment contained only the extensor pollicis longus tendon. The ER crossed over this tendon to attach to the fourth septum (Fig. 5), at an osseous prominence on the radius that separated the third and fourth compartments.
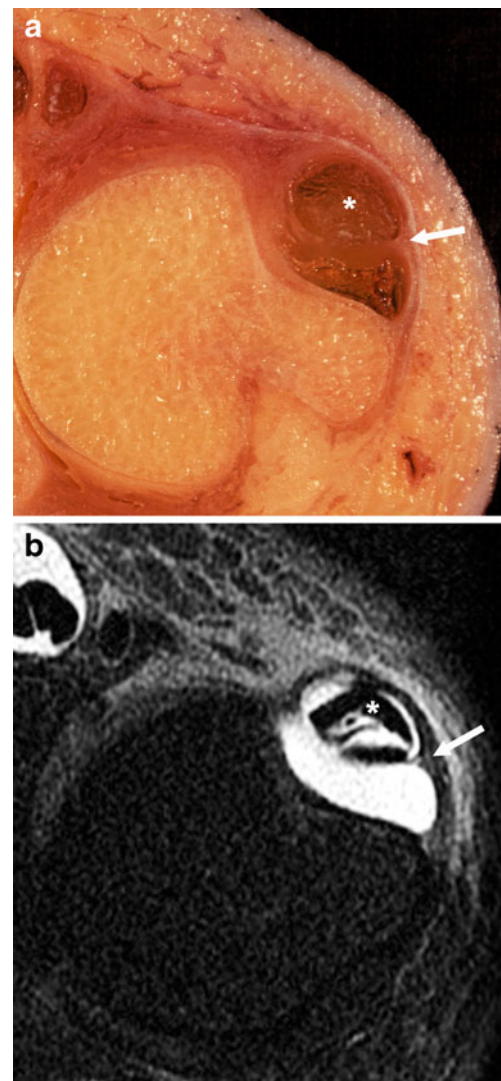

Fig. 8 Linea jugata. **a** Axial gross anatomical section after tenography and **b** corresponding T1-weighted fat-saturated image show the linea jugata (*arrow*) as a reinforcement at the ulnar insertion of the subsheath and help to prevent subluxation of the ECU tendon (*asterisk*) during supination

Fourth and fifth compartments (extensor digitorum communis and extensor indicis proprius tendons/extensor digiti minimi tendon)

At the level of the fourth and fifth compartments, the infratendinous retinaculum was well developed (Fig. 5), but narrower and shorter than the supratendinous portion, extending from the radiocarpal joint to the carpometacarpal joint. In our specimens, it blended with the dorsal wrist capsule and lay deep to the extensor digitorum communis and extensor indicis proprius tendons in the fourth. It also extended deep to the extensor digiti minimi tendon in the fifth compartment. The supratendinous portion crossed over the tendons of the fourth compartment, attaching to the dorsoulnar aspect of the radius to form the fifth fibrous septal attachment,

which was rejoined by fibers from the infratendinous portion, separating the fourth and fifth compartments (Fig. 6). The supratendinous and infratendinous portions continued around the extensor digiti minimi tendon, forming the fifth compartment.

At the level of the fourth compartment, the supratendinous portion of the ER could also be well-evaluated with ultrasound (Fig. 5) as a hypoechoic band relative to the tendons, both in transverse and sagittal images. However, we were unable to differentiate the infratendinous portion from the dorsal capsule using ultrasound.

Sixth compartment (extensor carpi ulnaris tendon)

After investing the fifth compartment, the two portions of the retinaculum blended again to form the sixth fibrous septum. This septum separated the extensor digiti minimi and the extensor carpi ulnaris (ECU) tendons with a variable pattern of osseous attachment to the radius. In 6 cases, we found a clear fibrous septum attaching to the dorsoulnar aspect of the radius, with a very close relationship to the fifth septal attachment site. In the other four cases, we found a common attachment with the fifth septum, forming a conjoined septum (Fig. 6). The sixth septum also extended over the proximal and distal carpal rows.

The ECU tendon was invested by its own fibrous subsheath, derived from the pars profunda of the antebrachial fascia, specifically formed by the infratendinous retinaculum (Fig. 7). Longitudinal fibers that reinforced the ulnar insertion of the subsheath were visible, which have been previously

designated the "linea jugata" (Fig. 8). These fibers extended from the ulnar styloid to merge with the supratendinous retinaculum and antebrachial fascia. However, native imaging did not demonstrate these fibers as well as tenography-enhanced images.

The supratendinous portion of the ER extended over the ECU tendon and its subsheath, blended with the volar antebrachial fascia, inserted into the sheath of the flexor carpi ulnaris tendon, and also attached to the triquetrum and pisiform (Fig. 9), but with no attachment to the ulna. At this level, the ER crossing over the ECU tendon could also be well visualized with ultrasound. The differentiation between the ER and the underlying subsheath was not very clear on the standard MR images, but could be accomplished with MR imaging following tenography and with ultrasound.

In the neutral and pronation positions, the ECU tendon was centered in the groove in the distal portion of the ulna in all our specimens. In full supination, ulnar displacement of the ECU tendon to the apex of the ulnar styloid at the ulnar border of the groove was found in 7 of our 10 specimens (Fig. 10).

Morphological changes in the ER after dorsiflexion of the wrist

In our 10 specimens, the width of the ER in neutral position ranged from 10.1 to 20.1 mm (mean ± SD, 13.56±3.08 mm), and the thickness of the ER varied from 1.1 to 2.4 mm (mean, 1.67±0.39 mm). With dorsiflexion of the wrist, the width of the ER ranged from 4.4 to 14.3 mm (mean, 8.68±2.93 mm), and the thickness from 1.6 to 2.8 mm (mean, 2.15±0.44 mm),
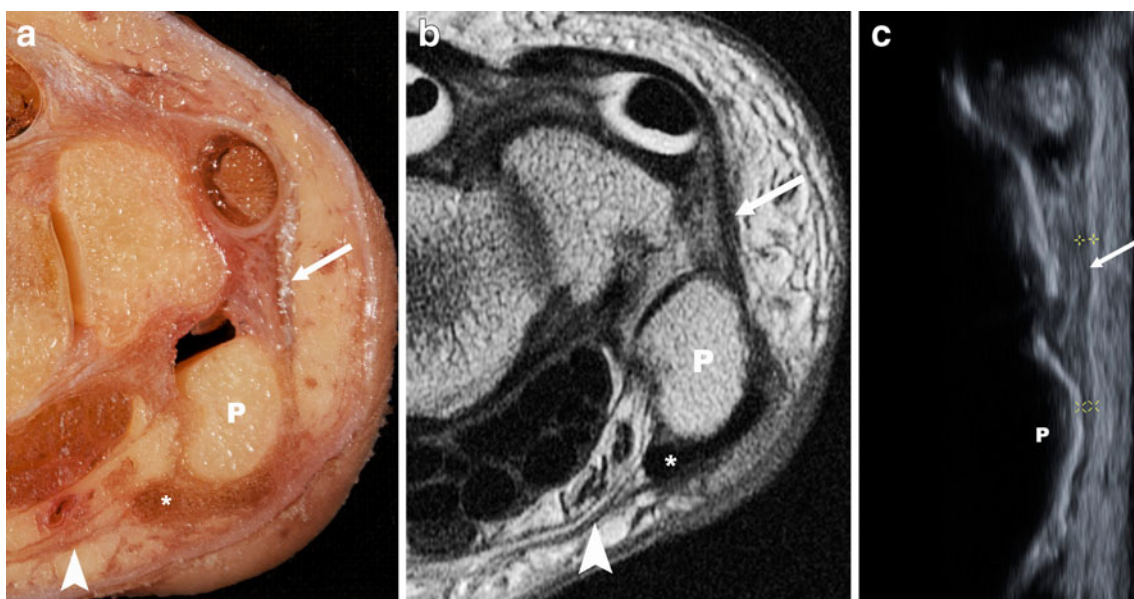

Fig. 9 Distal attachment of the ER on the ulnar side. **a** Axial gross anatomical section after tenography and **b** corresponding PD-weighted image and **c** ultrasound image show the retinaculum (*arrow*) attaching to the pisiform (*P*), inserting into the sheath of the flexor carpi ulnaris tendon (*asterisk*), and blending with the volar antebrachial fascia (*arrowhead*)
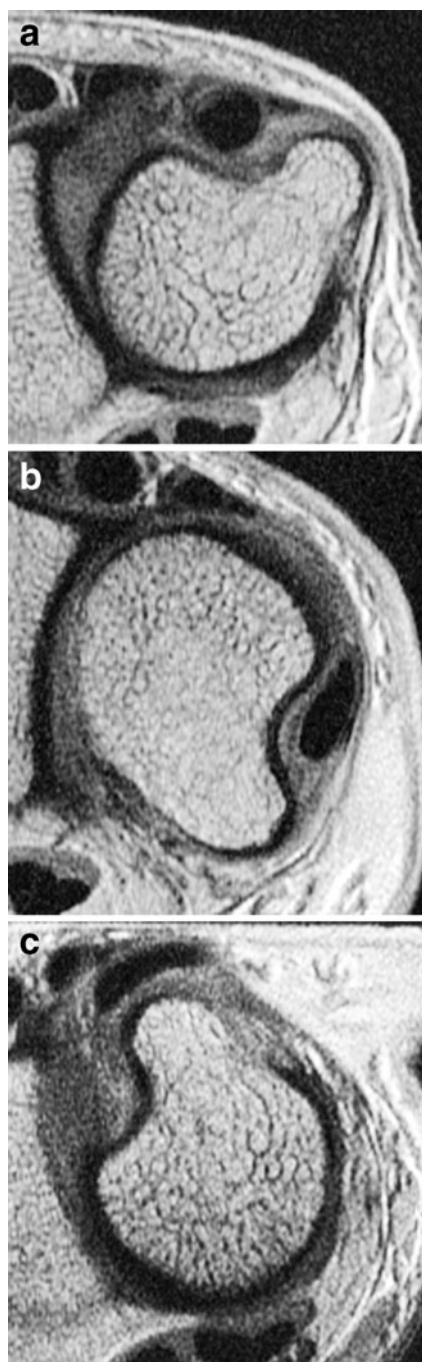
Fig. 10 Physiological displacement of the ECU tendon during supination. **a** Axial PD-weighted images show the normal positions of the ECU tendon during the neutral position, **b** pronation, and **c** supination. Note the normal tendency of the ECU tendon to sublux to the apex of the ulnar styloid at the ulnar border of the groove during supination

representing an increase from 13 % to 55 % (mean, 30 %) in thickness and a decrease from 25 % to 56 % (mean, 37 %) in width. Based on a two-tailed Student's t test, we found statistically significant difference both in the width ($p = 0.002$) and thickness ($p = 0.018$) of the ER before and after the dorsiflexion of the wrist.

All the specimens demonstrated morphological changes in the ER on MR images with dorsiflexion of the wrist: from an elongated fusiform appearance in the neutral position (Fig. 11), the ER shortened in proximal–distal width and became progressively thicker along the distal aspect, assuming a more rounded edge than in the neutral position. Specifically, its maximum thickness in its mid-point between the proximal and distal margins of the ER in the neutral position shifted more distally (Fig. 12) in the dorsiflexed position, coinciding with its contact portion with the dorsiflexed tendons of the fourth compartment. The proximal end of the ER kept static, remaining in the same position in relation to the radiocarpal joint, while the distal end moved proximal to it. These morphological changes correlated well with our observations in the gross anatomical studies performed in the dorsiflexion position (Fig. 12) in two specimens, even after the fourth compartment was distended with contrast agent (Fig. 13).

Discussion

The ER of the wrist can be used as a source of bone–retinaculum–bone autografts for wrist ligaments and pulley reconstructions of the fingers, which were first described in 1979 [4]. For this and other reasons, anatomical and biomechanical studies of the ER have been performed [1–3, 8, 9], including descriptions of its different septal attachments. Occasionally, an individual septum intrinsic to the first dorsal compartment could be found separating the APL and EPB tendons. Different anatomical studies have described the frequency of this septum as varying between 34 % and 77.5 % [8–13]. Our study revealed this septum in only one of ten cases. With regard to the anatomy and insertions of the septal attachments to the radius, Werther et al. [14] found that the fifth and sixth septa do not have attachments to the radius, while Taleisnik et al. [2] described bone attachments for both. Iwamoto et al. [3] found a small fifth septal attachment to the dorsoulnar aspect of the radius, but only a soft-tissue attachment of the sixth septum, with no osseous insertion. In our study, we found a clear fifth septal osseous attachment to the radius, separating the fourth and fifth compartments. Regarding the sixth septum, we found it attached closely to the fifth septum (6 cases) or coalesced with it (4 cases).

The two most detailed studies [2, 15] that supported our anatomical findings agreed that the anatomy of the sixth compartment containing the ECU tendon and its subsheath was unique and more complex. The supratendinous ER passes around and over the compartment to attach to the pisiform and triquetrum, and not directly to the ulna, an anatomical arrangement that allows free rotation of the forearm. The stability of the ECU tendon depends mainly on the integrity of its subsheath. If the ER is dissected or excised, the ECU tendon
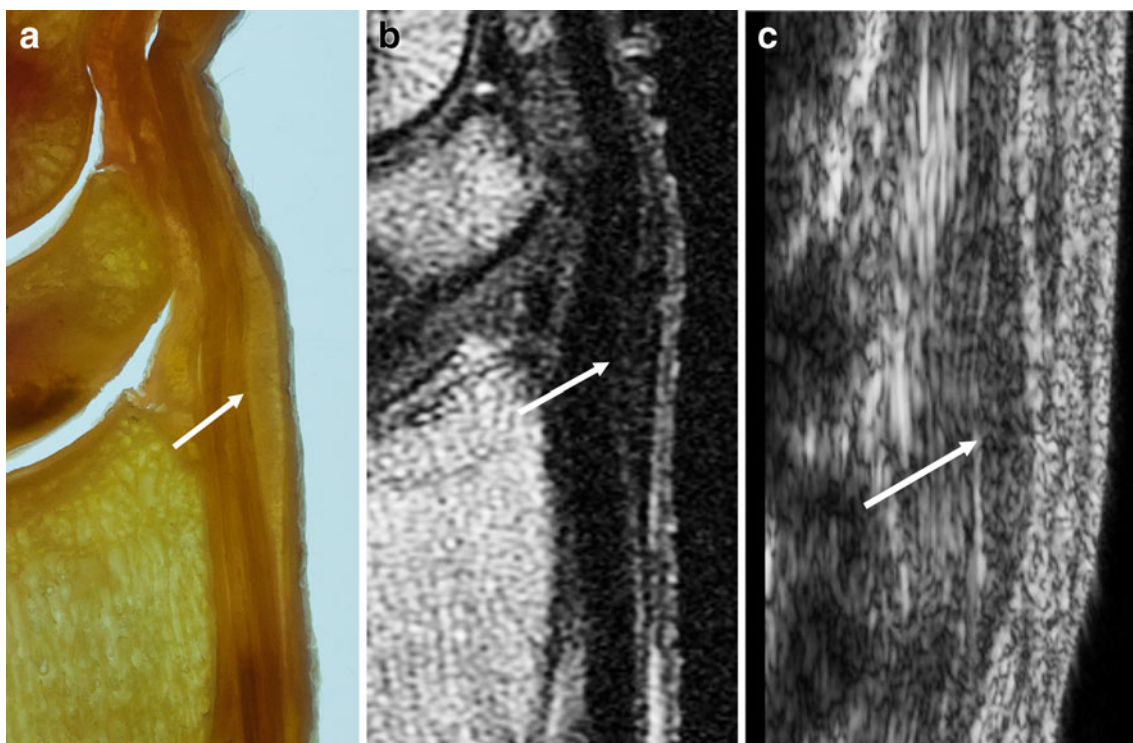
Fig. 11 Extensor retinaculum in the neutral position. **a** Sagittal gross anatomical section, **b** corresponding T1-weighted image and **c** ultrasound image show the fusiform morphology of the ER (*arrow*) in the neutral position

is not released (unlike the other extensor tendons), because the ECU tendon is maintained in place by its own fibrous subsheath. Alternatively, pathological displacement of the ECU tendon may occur as a consequence of a tear of its subsheath, even in the presence of an intact retinaculum. If the ER or the linea jugata, an important dynamic stabilizer that helps to prevent ECU tendon subluxation during full supination [2], is partially torn, instability of the ECU tendon without

a true tendon subluxation can occur [16]. However, physiological displacement of the ECU tendon to the apex of the ulnar border of the tendinous groove during wrist supination can be seen [17, 18], a finding that should not be regarded as pathological.

The linea jugata could be demonstrated neither with MR imaging without tenography nor with ultrasound in our study, possibly because of its longitudinal oblique fiber orientation
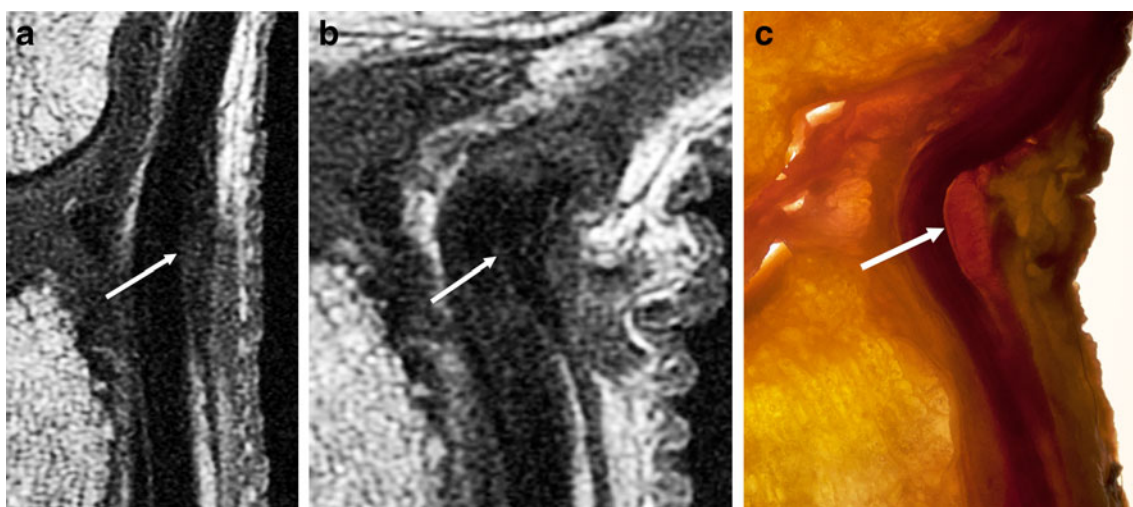

Fig. 12 Extensor retinaculum in the **a** neutral and **b**, **c** dorsiflexion positions at the level of the fourth compartment. T1-weighted images before (**a**) and after (**b**) dorsiflexion of the wrist, and corresponding

sagittal gross anatomical section in dorsiflexion (**c**) show the change in fusiform morphology of the ER (*arrow*) in the neutral position (**a**) to a configuration that presents gradual distal thickening in dorsiflexion (**b**, **c**)
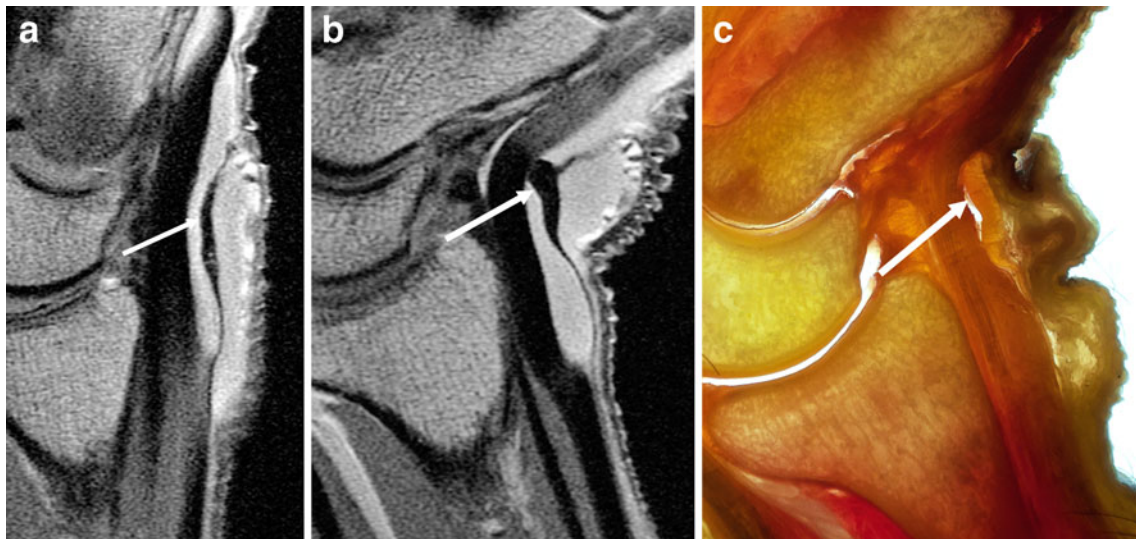
Fig. 13 Extensor retinaculum during **a** neutral and **b**, **c** dorsiflexion positions at the level of the fourth compartment. PD-weighted images before (**a**) and after (**b**) dorsiflexion of the wrist, and corresponding sagittal gross anatomical sections in dorsiflexion (**c**) show the same pattern of morphological changes in the ER (*arrow*), even after tenography. In this case, these findings might correlate with what occurs in patients with associated tenosynovitis

and its small size; however, in our gross anatomical sections and with MR tenography, it was visualized as a subtle thickened longitudinal layer reinforcing the medial (ulnar) border of the ECU subsheath extending from the base of the styloid process to the antebrachial fascia and supratendinous retinaculum.

In accordance with our study, Robertson et al. [19] noted the same ultrasound fusiform appearance of the ER in the neutral position in 100 retinacula from healthy adult volunteers. Regarding the echogenicity, all 100 retinacula were seen as hypoechoic tissue relative to the tendon owing to anisotropy. Such an appearance might be misdiagnosed as fluid, and consequently, tenosynovitis.

The ER is of paramount biomechanical function in dorsiflexion of the wrist, not only for tracking of the extensor tendons, but also to keep the apposition of the tendon and bone across the wrist joint preventing their bowstringing. However, as a consequence of this role, the ER may contribute to impingement of the extensor tendons.

As reported in the literature, the majority of cases of extensor tendon impingement describe a pathological thickening of the distal edge of the ER at surgical exploration [5–7]. Clinical signs and symptoms include triggering with extension, and localized dorsal swelling and tenderness, as well as pain with provocative maneuvers. Khazzam et al. [5] reported 5 patients with triggering of the extensor tendons at the level of the ER as a result of an anomalous muscle, intratendinous lesion, or synovial inflammation and tendon fraying. These investigators stated that multiple tendons sharing a limited space may contribute to the development of extensor tendon triggering, but they did not believe that there is a single unique

pathophysiological process, rather a multifactorial phenomenon. Wilson et al. [7] described a 26-year-old elite gymnast with a 4-year history of right dorsal wrist pain, particularly on hyperextension of the wrist during pommel horse training. They noticed an abutment of the extensor digitorum communis tendons against the thickened distal edge of the ER, and also stated that the presence of supernumerary tendons in the compartment could have exacerbated the patient's symptoms. VanHeest et al. [6] described 4 gymnasts, 2 platform divers, and 1 shot putter presenting wrist pain for several weeks or months worsened by wrist extension, and exacerbated during a particular load-bearing activity. Tenosynovitis and a thickened border of the ER were seen in all patients at the time of the surgery.

The distal thickened border of the ER observed during dorsiflexion of the wrist could be the result of impingement of the extensor tendons of the fourth compartment, since this distal margin is the contact portion with the most angulated and curved excursion of the dorsiflexed tendons. The impingement would be caused by a vector force and tension created by the extensor tendons during wrist dorsiflexion that acts against the distal border of the restraining ER. These morphological changes that occur during dorsiflexion of the wrist were present even after tenography. In this case, it might be correlated with the distended tendon sheath that occurs in patients with tenosynovitis.

Utilizing dynamic ultrasound, we dorsiflexed the wrist with the transducer in a sagittal position over the fourth compartment at 45° to 60° degrees of dorsiflexion, owing to the constrained space in the dorsiflexed wrist, despite using the small footprint of a hockey stick transducer. Nevertheless,

even with limited dorsiflexion, we noticed the same pattern of change in the shape of the ER as seen on the MR imaging and gross slices study.

Our study had several limitations. Owing to the small number of specimens, we did not encounter many anatomical variations of the ER. Additionally, our donors were of advanced age, a common limitation of cadaveric studies, and may have had a smaller range of motion compared with a younger population. However, it is unlikely that the morphology of the ER that was observed in the neutral and dorsiflexion positions in our study are significantly different from an in vivo pattern. The use of cadaveric specimens allowed longer MRI acquisition times and dynamic positioning, differing from usual clinical practice. We used a knee coil to allow adequate space for additional positions of the wrist other than neutral positioning, which would not be possible with a dedicated wrist coil. Our findings may be useful in the further investigation of the ER in symptomatic athletes with extensor compartment pathology.

We consider high-resolution MR imaging to be the best imaging method to evaluate the ER, allowing analysis of its different septal attachments and nearby tendons and sheaths. Ultrasound is also a good diagnostic method, with its inherent low cost and dynamic nature, although it is limited in the evaluation of the retinacular attachments, and is operator-dependent.

Retinacular impingement of the extensor tendons has been described as a rare clinical entity. Our findings implicate physiological factors that may explain the pathogenesis of such impingement. With wrist extension, the extensor tendons create a vector force that acts against the distal border of the restraining ER, causing its distal thickening. However, repetitive dorsiflexion movements may cause a chronic thickening of the ER, as seen in athletes affected by this pathological feature. Future studies are required to further evaluate any potential consequence of this finding in a clinical setting.

References

1. Palmer AK, Skahen JR, Werner FW, Glisson RR. The extensor retinaculum of the wrist: an anatomical and biomechanical study. J Hand Surg (Br). 1985;10(1):11–6.

2. Taleisnik JT, Gelberman RH, Miller BW, Szabo RM. The extensor retinaculum of the wrist. J Hand Surg. 1984;9(4):495–501.

3. Iwamoto A, Morris RP, Andersen C, Patterson RM, Viegas SF. An anatomic and biomechanic study of the wrist extensor retinaculum septa and tendon compartments. J Hand Surg. 2006;31(6):896–903.

4. Lister GD. Reconstruction of pulleys employing extensor retinaculum. J Hand Surg Am. 1979;4(5):461–4.

5. Khazzam M, Patillo D, Gainor BJ. Extensor tendon triggering by impingement on the extensor retinaculum: a report of 5 cases. J Hand Surg. 2008;33(8):1397–400.

6. VanHeest A, Luger NM, House JH, Vener M. Extensor retinaculum impingement in the athlete: a new diagnosis. Am J Sports Med. 2007;35(12):2126–30.

7. Wilson SM, Dubert T, Rozenblat M. Extensor tendon impingement in a gymnast. J Hand Surg (Br). 2006;31(1):66–7.

8. Jackson WT, Viegas SF, Coon TM, Stimpson KD, Frogameni AD, Simpson JM. Anatomical variations in the first extensor compartment of the wrist. A clinical and anatomical study. J Bone Joint Surg Am. 1986;68(6):923–6.

9. Gonzalez MH, Sohlberg R, Brown A, Weinzweig N. The first dorsal extensor compartment: an anatomic study. J Hand Surg [Am]. 1995;20(4):657–60.

10. Shiraishi N, Matsumura G. Anatomical variations of the extensor pollicis brevis tendon and abductor pollicis longus tendon-relation to tenosynovectomy. Okajimas Folia Anat Jpn. 2005;82(1):25–9.

11. Leslie BM, Ericson Jr WB, Morehead JR. Incidence of a septum within the first dorsal compartment of the wrist. J Hand Surg [Am]. 1990;15(1):88–91.

12. Mahakkanukrauh P, Mahakkanukrauh C. Incidence of a septum in the first dorsal compartment and its effects on therapy of de Quervain's disease. Clin Anat. 2000;13(3):195–8.

13. Choi SJ, Ahn JH, Lee YJ, Ryu DS, Lee JH, Jung SM, et al. de Quervain disease: US identification of anatomic variations in the first extensor compartment with an emphasis on subcompartmentalization. Radiology. 2011;260(2):480–6.

14. Werther JR, Guelmi K, Mazodier F, Doursounian L. Use of the extensor retinaculum as a donor site for bone-ligament-bone grafts. Surg Radiol Anat. 2001;23(5):295–9.

15. Spinner M, Kaplan EB. Extensor carpi ulnaris. Its relationship to the stability of the distal radio-ulnar joint. Clin Orthop Relat Res. 1970;68:124–9.

16. Carneiro RS, Fontana R, Mazzer N. Ulnar wrist pain in athletes caused by erosion of the floor of the sixth dorsal compartment: a case series. Am J Sports Med. 2005;33(12):1910–3.

17. Pfirrmann CW, Theumann NH, Chung CB, Botte MJ, Trudell DJ, Resnick D. What happens to the triangular fibrocartilage complex during pronation and supination of the forearm? Analysis of its morphology and diagnostic assessment with MR arthrography. Skeletal Radiol. 2001;30(12):677–85.

18. Lee KS, Ablove RH, Singh S, De Smet AA, Haaland B, Fine JP. Ultrasound imaging of normal displacement of the extensor carpi ulnaris tendon within the ulnar groove in 12 forearm-wrist positions. AJR. 2009;193(3):651–5.

19. Robertson BL, Jamadar DA, Jacobson JA, Kalume-Brigido M, Caoili EM, Margaliot Z, et al. Extensor retinaculum of the wrist: sonographic characterization and pseudotenosynovitis appearance. AJR Am J Roentgenol. 2007;188(1):198–202.